Temperature-based tuning of magnetic particle separation by on-chip free-flow magnetophoresis

Mark D. TARN [1,*], Damien ROBERT [2], Sally A. PEYMAN [1], Alexander ILES [1], Claire WILHELM [2], Nicole PAMME [1]

* Corresponding author: Tel.: +44 (0)1482 465476; Fax: +44 (0)1482 466416; Email: m.tarn@chem.hull.ac.uk
1: Department of Chemistry, The University of Hull, UK
2: Université Paris-Diderot, France

Abstract Free-flow magnetophoresis provides a fast and efficient means of continuous flow magnetic separation for the detection of biological analytes, due to the wide variety of magnetic particle surface properties available for binding specific targets. Here, we investigate the effect of temperature changes on the deflection behaviour of magnetic particles in a microfluidic magnetophoresis separation chamber. It was found that the extent of deflection was greatly increased at higher temperatures due to decreased solution viscosity and thus reduced resistance against particle motion. This concept was used to improve the resolution of the separation of 2.8 μm and 1 μm diameter magnetic particles. Hence, controlling the temperature of the separation system provides a simple but highly effective means of enhancing magnetic separation efficiency. This concept could also be applied to the temperature-based tuning of microparticle trajectories in many others types of continuous flow processes, such as those using optical, electrical or acoustic forces.

Keywords: Magnetophoresis, Magnetic Particles, Separation, Temperature Dependence, Viscosity, Continuous Flow

1. Introduction

Magnetic particles have become increasingly popular in recent years as solid supports in biomedical and chemical applications (Gijs, 2004; Pamme, 2006; Pankhurst et al., 2003; Verpoorte, 2003). They can be fabricated from a number of materials, with polystyrene being a common choice, and usually contain a core of iron oxide nanoparticles that renders them superparamagnetic (Fig. 1a). Thus, such particles are only magnetised in the presence of a magnetic field; when the field is removed they redisperse into solution. Available sizes range from tens of nanometres to several micrometres, and the surfaces can be functionalised to allow the specific binding of a target material for its removal from a sample solution (Fig. 1b). The general procedure is depicted in Fig. 2. Appropriately functionalised particles are added to a sample mixture. After binding to the desired analyte

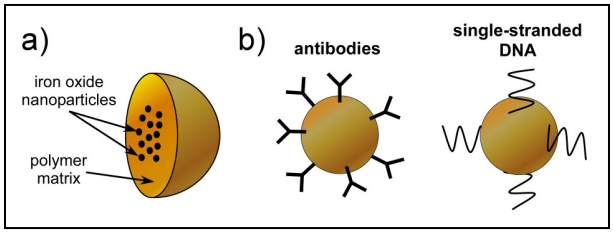

Fig. 1. (a) Cross-section of a magnetic particle, featuring a core of iron oxide nanoparticles. (b) Examples of some particle surface functionalities.

they are trapped in a magnetic field, the supernatant is removed and replaced with fresh buffer solution. The particles must then be washed several times to ensure any unbound material is removed from the particle surface. However, whilst this is an effective method of separation, it is also time-consuming and labour-intensive due to the number of washing steps required.

Continuous flow separations (Kersaudy-Kerhoas et al., 2008; Pamme, 2007) of magnetic particles and magnetically-labelled cells (Xia et al., 2006) have been of great

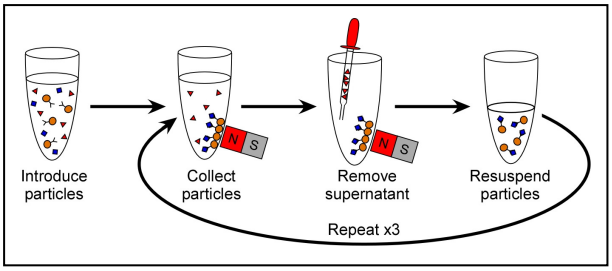

Fig. 2. Conventional magnetic particle separation methodology, hampered by time consuming and laborious washing steps.

interest due to their ability to combine the separation and washing steps into one process, thus eliminating some of the inefficiencies of normal batch-based methods. Such approaches have included quadrupole magnetic field-flow fractionation (Carpino et al., 2005) and split-flow thin fractionation (SPLITT) (Fuh et al., 2003). In recent years, the integration of continuous flow magnetic separation techniques into microfluidic systems has shown great potential (Gijs, 2004; Pamme, 2006). These systems incorporate the magnetic separation of the bound target molecules from the sample solution for detection downstream. Such techniques have included the separation and detection of dengue virus in serum (Chang et al., 2008), the purification of *E.coli* cells (Adams et al., 2008), as well as our on-chip free-flow magnetophoresis device for particle separation and cell sorting (Pamme et al., 2006; Pamme and Manz, 2004; Pamme and Wilhelm, 2006).

On-chip free-flow magnetophoresis is a fast and efficient separation method (Fig. 3) in which magnetic particles, following a laminar flow regime, are introduced into a separation chamber. They are deflected from their paths by the application of a perpendicular magnetic field and collected as they leave the chamber via different outlets. Hence, the extent of magnetic particle deflection is an important parameter for performing efficient separations.

Magnetic deflection can be affected by adjusting several parameters including the magnetic field, the size of the particles and their magnetic properties, as well as the viscosity of the buffer solution. It is well known that changes in solution temperature alters fluid viscosity, however the effect of

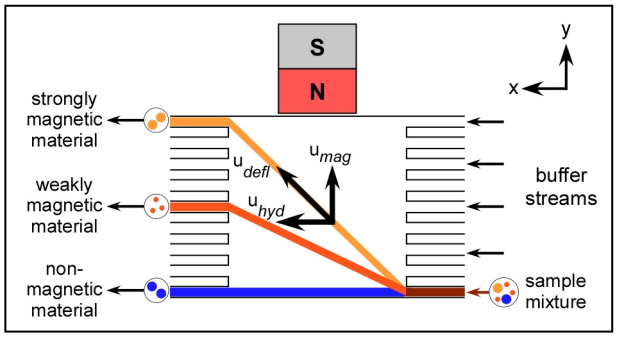

Fig. 3. The principle of free-flow magnetophoresis. Magnetic particles are introduced into a separation chamber and deflected to varying degrees by an applied magnetic field, thus achieving separation in continuous flow and in an automated fashion.

temperature on magnetic deflection has not been investigated.

Here, we explore the result of changing temperature on particle deflection behaviour, and on the resolution of particle separation.

2. Theory

2.1 Magnetic separation in flow

The principle of free-flow magnetophoresis is illustrated in Fig 3. Laminar flow is generated across a separation chamber in the x-direction, and magnetic particles are introduced from one corner of the chamber, travelling in the direction of flow with a hydrodynamic velocity of $\mathbf{u_{hyd}}$ (m s^{-1}). A magnetic field is generated in the y-direction, perpendicular to the direction of flow, via an external magnet. The particles experience an attractive force to the magnetic field and migrate towards the region of highest flux density with a magnetically-induced velocity of $\mathbf{u_{mag}}$ (m s^{-1}), whilst being subjected to hydrodynamic flow in the x-direction. The result of this is a deflection of the particles from the direction of flow, with the observed velocity, $\mathbf{u_{defl}}$ (m s^{-1}), being the sum of the $\mathbf{u_{mag}}$ and $\mathbf{u_{hyd}}$ vectors (Pamme and Manz, 2004):

$$\mathbf{u_{defl}} = \mathbf{u_{mag}} + \mathbf{u_{hyd}} \quad (1)$$

When the hydrodynamic flow rate is fixed, i.e. $\mathbf{u_{hyd}}$ remains constant, the extent of deflection depends only upon the value of $\mathbf{u_{mag}}$.

The force of magnetic attraction experienced by the particles in a magnetic field, $\mathbf{F_{mag}}$ in N, is a function of the magnetic susceptibilities (dimensionless) of the particle, χ_p, and the surrounding medium, χ_m, the volume of magnetic material in the particle, V_m in m^3, the strength and gradient of the magnetic field, $(\mathbf{B}\cdot\nabla)\mathbf{B}$ in $T^2\ m^{-1}$, as well as the permeability of free space, μ_0 (4π x 10^{-7} H m^{-1}) (Pamme, 2006).

$$\mathbf{F_{mag}} = \frac{(\chi_p - \chi_m)V_m(\mathbf{B}\cdot\nabla)\mathbf{B}}{\mu_0} \quad (2)$$

$\mathbf{F_{mag}}$ is opposed by an equal viscous drag force, $\mathbf{F_{vis}} = 6\pi\eta r\mathbf{u_{mag}}$, and thus $\mathbf{u_{mag}}$ can be expressed as:

$$\mathbf{u_{mag}} = \frac{\mathbf{F_{mag}}}{6\pi\eta r} \quad (3)$$

where η is the absolute viscosity of the medium in kg m^{-1} s^{-1}, and r is the radius of the particle in m.

For a given setup, the magnetic field, the magnetic susceptibilities, and the velocity of a particle due to hydrodynamic flow are constant. Hence, the extent of deflection experienced by a particle depends on its size (radius), the volume and type of magnetic material it contains, and the viscosity of the surrounding media.

2.2 Effect of temperature on viscosity

As shown in equation (3), the value of $\mathbf{u_{mag}}$ is inversely proportional to the viscosity of the solution and hence a change in viscosity will have an effect on the extent of deflection of a particle in the magnetic field. One of the factors influencing viscosity is the temperature of the medium, with the relationship between the two given by equation (4) (Moore, 1962):

$$\eta = A\exp(\Delta E_{vis} / RT) \quad (4)$$

where A is a constant, ΔE_{vis} is the activation energy for viscous flow in J mol^{-1}, R is the gas constant of 8.315 J K^{-1} mol^{-1}, and T is the temperature in K. This relationship demonstrates that as the temperature of a solution is increased, in this case 0.1x glycine saline buffer, the viscosity decreases (Table 1), which should result in a greater degree of particle deflection according to equation (3).

Table 1. Measured viscosity values of 0.1x glycine saline buffer solution over a range of temperatures.

Temp. / °C	Viscosity / x 10^{-3} kg m^{-1} s^{-1}
5	1.522 ± 0.005
10	1.322 ± 0.005
20	1.023 ± 0.007
30	0.810 ± 0.007
40	0.670 ± 0.004
50	0.554 ± 0.013

3. Experimental

3.1 Preparation of particle suspensions

Superparamagnetic particles of 2.8 μm diameter featuring epoxy surface groups (Dynabeads M-270 Epoxy) were purchased from Invitrogen (Paisley, UK) and prepared according to the manufacturer's instructions. 3 mg of dry particles (2 x 10^8 beads) were dispersed in 1 mL phosphate buffered saline. The particles were collected via a magnet, the supernatant removed and fresh buffer solution added. This washing step was repeated twice more, the particles resuspended in 1 mL of 10x concentrated glycine saline (100 mM glycine, 150 mM sodium chloride, pH 8.3) and the suspension incubated overnight to allow the glycine to deactivate the reactive epoxy surface groups and to render the surface negatively charged. 10 μL of the suspension was added to 990 μL of 1x glycine saline buffer (10 mM glycine, 15 mM sodium chloride, pH 8.3) to give a final particle concentration of 2 x 10^6 particles mL^{-1}; the suspension was stored at 4 °C.

1 μm diameter superparamagnetic particles featuring carboxylic acid surface groups (Dynabeads MyOne Carboxylic Acid) were also purchased from Invitrogen as an aqueous suspension of 1 x 10^{10} particles mL^{-1}. 20 μL of the stock solution was added to 980 μL of 10x glycine saline and incubated overnight. 10 μL of this suspension was then diluted in 990 μL of 1x glycine saline to give a final

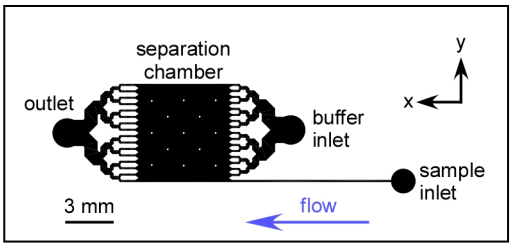

Fig. 4. Schematic of the magnetophoresis chip design, featuring a separation chamber, a single sample inlet, 16 buffer inlet channels and 16 outlet channels.

concentration of 2 x 10^6 particles mL^{-1}. The suspension was stored at 4 °C.

3.2 Fabrication and setup of the microfluidic device

The microfluidic chip design shown in Fig. 4 featured a 6 mm by 6 mm central separation chamber, with 13 diamond-shaped posts used to support the chamber roof. 16 buffer inlet channels and a single sample inlet channel were situated opposite 16 outlet channels, with each channel being 100 µm in width. The buffer inlets featured a branching channel system to allow introduction of buffer solution from a single reservoir, with the outlets similarly branched to allow pumping via single withdrawing syringe. The branched outlet system was suitable for proof-of-principle experiments as the recombining of any separated particle populations was not a concern.

The design was fabricated in glass using conventional photolithography and wet etching methods (McCreedy, 2000). A 1 mm thick glass wafer, coated with a chromium layer and photoresist layer (B270 glass, Telic, Valencia, CA, USA) was exposed to UV light through a photomask featuring the chip design (JD Photo-Tools, Lancashire, UK) for 60 s. The photoresist was subsequently developed (Microposit Developer, Chestech Ltd., Rugby, Warwickshire, UK) to remove the exposed pattern, and the revealed chromium layer etched away (Microposit Chrome Etch 18, Chestech Ltd.) to leave the design visible on the glass surface. The exposed glass was etched to a depth of 20 µm with hydrofluoric acid, then access holes (1 mm diameter) were drilled into the wafer. The photoresist and chromium layers were removed entirely and

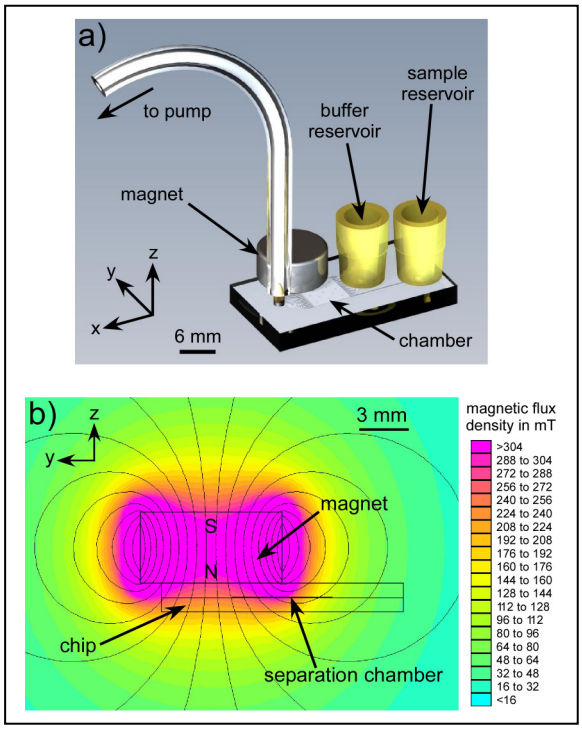

Fig. 5. (a) Setup of the microfluidic device, illustrating the placement of reservoirs, tubing, and the cylindrical magnet. (b) Side-view of the magnetic field generated across the separation chamber.

the etched plate was thermally bonded to a cover plate of the same glass type.

Buffer and sample reservoirs were fabricated from plastic pipette tips and glued over the inlet holes using epoxy resin (Fig. 5a). A 1 cm length of PEEK tubing (0.5 mm i.d., 1.6 mm o.d., Cole-Parmer, London, UK) was glued into the outlet hole and interfaced to a 5 mL syringe via 6 cm long Tygon tubing (1.0 mm i.d., 1.8 mm o.d., Cole Parmer). A syringe withdrawal rate of 400 µL h^{-1} (0.93 mm s^{-1}) was achieved using a syringe pump (Pump 11 Plus, Harvard Apparatus, Kent, UK).

A 10 mm x 5 mm cylindrical Neodymium-Iron-Boron magnet (Magnet Sales, Swindon, UK) was placed on the chip such that it covered half of the separation chamber, as shown in Fig. 5. A Hall sensor (LOHET II, RS Components, Corby, UK) was used to determine the magnetic flux density, **B**, at the surface of the magnet and at the sample inlet, which were measured at >320 mT and 28 mT, respectively. The magnetic flux density over the chip was simulated (Fig. 5b) using FEMM 4.0 freeware (http://femm.foster-miller.net)

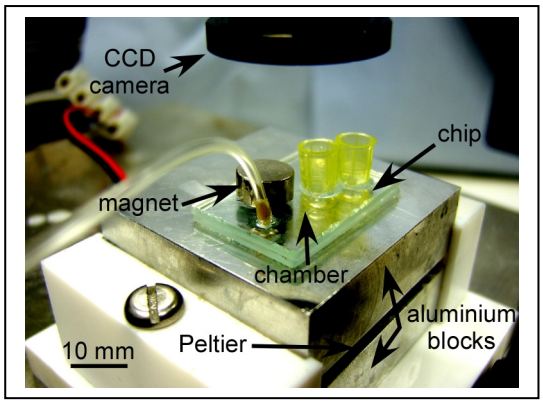

Fig. 6. Chip setup for temperature experiments. The chip was placed onto a Peltier heater sandwiched between aluminium blocks. A CCD camera was used for visualisation of the particles.

and illustrates the field gradient over the separation chamber.

The temperature of the microfluidic chip was controlled by fixing it to a Peltier element (Thermo Module 127 TEC1-12708, Akizukidenshi, Tokyo, Japan) sandwiched between two aluminium blocks that acted as heatsinks (Fig. 6). The voltage supplied to the Peltier element was varied using a DC power supply (SM5020, Digimess, Reading, Berkshire, UK) and when low temperatures were required the setup was fixed to a computer heatsink and cooling fan to help cool the system. The temperature of the chip was measured using a combination of a hand-held infrared temperature sensor (Precision Gold, Maplin Electronics, Barnsley, South Yorkshire, UK), and a thermocouple (TM-301 Dual Thermometer, AS ONE, Japan).

Visualisation of the separation chamber was achieved using an overhead zoom CCD camera (PV10, Olympus, Japan).

3.3 Experimental procedures

The chip was pretreated by flushing with an aqueous base to render the glass surface negative, thus preventing sticking of the particles, followed by flushing with deionised water and finally 0.1x glycine saline buffer (1 mM glycine, 1.5 mM sodium chloride, pH 8.3) for 15 min each. Particle suspensions were diluted 1 in 10 with 0.1x glycine saline prior to experiments to give final working concentrations of 2 x 10^5 particles mL^{-1}, and introduced into the sample reservoir in place of the buffer solution. Withdrawal rates of 400 $\mu L\ h^{-1}$ were applied to pull the buffer solution and the particle suspension through the chamber.

The outlets of the microfluidic chamber were numbered 1 to 16, with outlet 1 being directly opposite the particle inlet and outlet 16 being furthest away. At each temperature, with no magnet present, the particles exited the chamber through outlet 1.

Two series of experiments were undertaken using this setup, the first being a study of the deflection behaviour of M-270 particles over a range of temperatures. Here, the percentage number of particles exiting each outlet was counted over 4 minutes at temperatures of 5, 15, 20, 43 and 50 °C. In the second series of experiments, the effect of temperature on the separation of a mixture of M-270 and MyOne particles was examined, again by determining the percentage of particles exiting each outlet, at 5, 20 and 50 °C.

3.4 Particle trajectory simulations

The expected deflection paths of the particles were simulated using a program written in-house. The model was based on a map of the magnetic field gradient across the separation chamber, as described by Pamme and Wilhelm, 2006), combined with information on flow rate, temperature and particle type to perform the calculations.

4. Results and discussion

4.1 Temperature dependence of magnetic particle deflection

The effect of temperature changes on particle deflection in a magnetophoresis chip was investigated. This was achieved by deflecting Dynabeads M-270 Epoxy particles through the separation chamber at several different temperatures to vary the solution viscosity, as described in Section 2.2. The results for the deflection behaviour of the particles are shown in Fig. 7.

As anticipated by equations (3) and (4), at the lowest temperature of 5 °C the particles exhibited the least amount of deflection, either exiting via outlet 2 (an average deflection

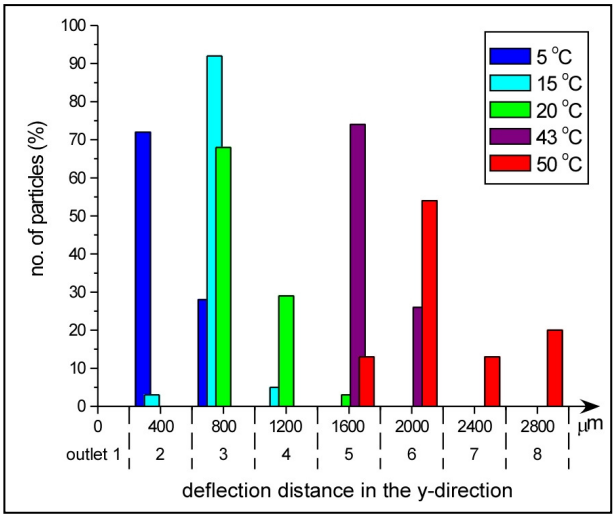

Fig. 7. The percentage of M-270 particles exiting the separation chamber via several outlets, and the corresponding deflection distances, at different temperatures.

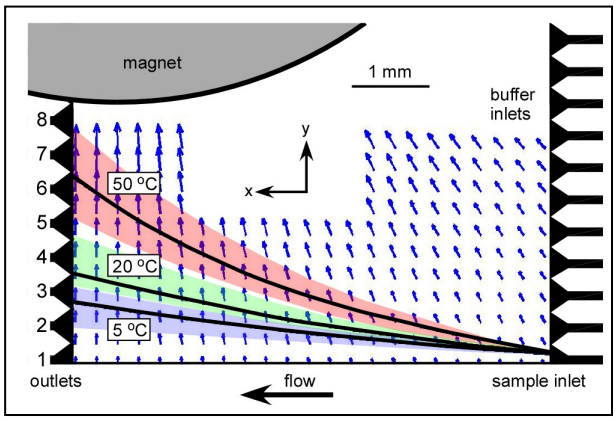

Fig. 8. Simulated trajectories (black lines) of the M-270 particles through the separation chamber at three temperatures. The coloured regions indicate the range of paths taken by the particles during the experiments.

distance of 400 µm) or outlet 3 (800 µm). At 15 °C the particles showed a slight increase in deflection distance as they exited mostly at outlet 3, while at 20 °C the majority of particles still left the chamber via outlet 3, but more particles now left through outlet 4 (1200 µm) and some even through outlet 5 (1600 µm). Greatly increasing the temperature to 43 °C resulted in a large increase in deflection distance, with over 70 % of particles exiting via outlet 5 and the rest via outlet 6 (2000 µm), whilst at the highest experimental temperature, 50 °C, most particles left through outlet 6, with some even reaching as far as outlet 8 (2800 µm).

The spread of particles over several exits at each temperature was caused by (1) differences in their position upon entering the chamber through the 230 µm wide inlet channel, (2) differences in particle velocity due to the parabolic flow profile, and (3) differences in magnetite content within the particle population. The spread was generally consistent throughout the temperature range, with particles mostly exiting over two or three outlets. The exception to this was at 50 °C where some of the particles were found to stick briefly to the chamber surface, thus affecting their relative $\mathbf{u}_{mag}$ and $\mathbf{u}_{hyd}$ velocities.

Simulations of the particle paths were run at 5, 20 and 50 °C using the program described in Section 3.4, to compare the theoretical and experimental results. The simulations were combined into Fig. 8, in which the solid black lines show the theoretically expected paths, while the coloured regions surrounding each line indicate the spread of particles observed during the experiments. The arrows shown in the chamber indicate the direction and magnitude of the magnetic field gradient at that point. An arrow 1 mm in length on the scale given in the figure is equivalent to a field gradient of 60 T m^{-1}, and hence typical values in the chamber are around 10 T m^{-1}. As would be expected, the gradient is greatest nearer the magnet surface, resulting in the curved paths the particles take as they traverse the chamber. Fig. 8 shows that the experimental results compared very well with the expected values.

These experiments clearly demonstrate that when the only parameter changed was the temperature and therefore viscosity, the paths of the particles were greatly affected. Increasing the temperature reduced the viscosity of the solution, allowing particles to migrate through the fluid with less resistance and thus achieve a larger deflection distance.

4.2 Separation of two particle populations

Having established the effect of temperature on the particle deflection behaviour, an investigation was undertaken to determine the effect of temperature on the resolution of a magnetophoretic separation.

A mixture of 2.8 µm (M-270) and 1 µm

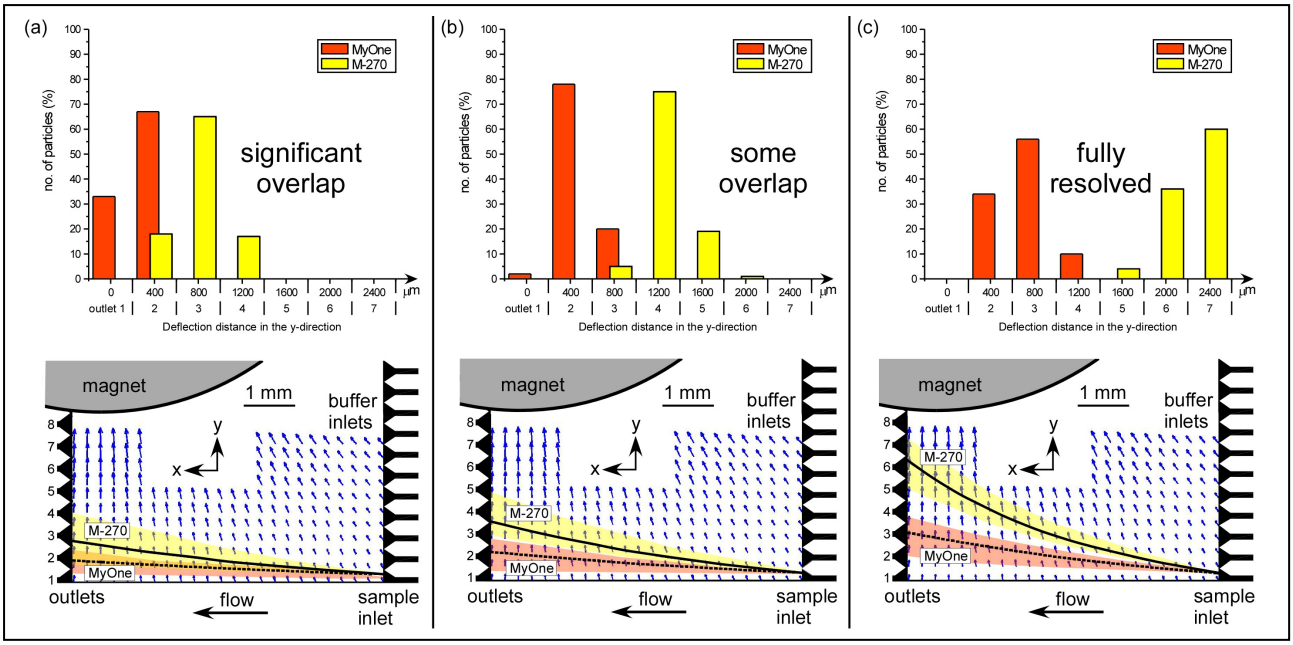

Fig. 9. Separation of Dynabeads MyOne (1 µm) and M-270 (2.8 µm) particles at (a) 5 °C, (b) 20 °C, and (c) 50 °C. The corresponding simulations in the bottom row illustrate the expected particle paths, while the coloured regions show the range of experimental paths taken by the particles.

(MyOne) diameter magnetic particles was introduced into the sample inlet of the magnetophoresis chip at temperatures of 5, 20 and 50 °C. The two particle types were separated due to their differences in magnetic content, with the 2.8 µm particles containing a greater volume of magnetic material that resulted in larger magnetic forces (equation (2)). The results of the separation at the three temperatures are shown in Fig. 9.

Changes in temperature affected both particle types, but due to their greater magnetic content, the M-270 particles experienced a greater difference in deflection behaviour than their smaller counterparts. At 5 °C, the majority of M-270 particles were deflected into outlet 3 while the MyOne particles mostly exited the chamber via outlet 2. However, there was significant overlap between the two populations at outlet 2. Increasing the temperature to 20 °C improved the separation, with most of the M-270 particles exiting through outlet 4 and the MyOne particles at outlet 2, though there was still a small amount of overlap at outlet 3. A full separation of the particles was achieved at 50 °C, with the M-270 particles exiting via outlets 5 to 7, and the MyOne particles at outlets 2 to 4. Thus, increasing the temperature of the system, and so decreasing the buffer solution viscosity, successfully increased the resolution of the separation.

As in Section 4.1, simulations were run to compare the experimental results to the expected particle paths (Fig. 9). The data generally compared well, particularly at lower temperatures where at 5 and 20 °C the majority of particles exited the chamber at the expected outlet. The simulation at 50 °C suggested the particles would exit the chamber via outlet 6, but very close to outlet 7. This was reflected by the majority of particles exiting via outlets 6 and 7 in the experiments.

5. Conclusions

The effect of temperature on the deflection behaviour of magnetic particles was investigated in an on-chip free-flow magnetophoresis system. As the temperature was increased, the viscosity of the buffer solution was reduced, leading to a marked rise in the extent to which the particles were deflected from the direction of laminar flow by a magnetic field. Furthermore, a separation of two particle populations was performed over a range of temperatures, with the resolution of the separation found to increase with

increasing temperature.

The results illustrate the importance of controlling the temperature of continuous flow separation systems to avoid discrepancies in run-to-run repeatability. They also demonstrate a simple method for improving a separation by simply increasing the temperature. Careful control of the system temperature should also allow the tuning of the device such that the trajectory of one particle type could be directed to a specified outlet to allow its collection and analysis. These findings are of particular interest not only to researchers dealing with free-flow magnetophoresis, but also to those utilising various other forces including optical, ultrasound, and dielectrophoresis among others for microfluidic continuous flow operations.

Acknowledgements

The authors would like to acknowledge the Engineering and Physical Sciences Research Council (EPSRC) for funding.

References

Adams, J.D., Kim, U., Soh, H.T., 2008. Multitarget magnetic activated cell sorter. Proc. Natl. Acad. Sci. USA 105, 18165-18170.

Carpino, F., Moore, L.R., Zborowski, M., Chalmers, J.J., Williams, P.S., 2005. Analysis of magnetic nanoparticles using quadrupole magnetic field-flow fractionation. J. Magn. Magn. Mater. 293, 546-552.

Chang, W.S., Shang, H., Perera, R.M., Lok, S.M., Sedlak, D., Kuhn, R.J., Lee, G.U., 2008. Rapid detection of dengue virus in serum using magnetic separation and fluorescence detection. Analyst 133, 233-240.

Fuh, C.B., Tsai, H.Y., Lai, J.Z., 2003. Development of magnetic split-flow thin fractionation for continuous particle separation. Anal. Chim. Acta 497, 115-122.

Gijs, M.A.M., 2004. Magnetic bead handling on-chip: new opportunities for analytical applications. Microfluid. Nanofluid 1, 22-40.

Kersaudy-Kerhoas, M., Dhariwal, R., Desmulliez, M.P.Y., 2008. Recent advances in microparticle continuous separation. IET Nanobiotechnol. 2, 1-13.

McCreedy, T., 2000. Fabrication techniques and materials commonly used for the production of microreactors and micro total analytical systems. Trends in Anal. Chem. 19, 396-401.

Moore, W.J., 1962. Physical Chemistry, 4th edn., Longmans Green & Co. Ltd., London (Chapter 17) p. 723.

Pamme, N., 2006. Magnetism and microfluidics. Lab Chip 6, 24-38.

Pamme, N., 2007. Continuous flow separations in microfluidic devices. Lab Chip 7, 1644-1659.

Pamme, N., Eijkel, J.C.T., Manz, A., 2006. On-chip free-flow magnetophoresis: Separation and detection of mixtures of magnetic particles in continuous flow. J. Magn. Magn. Mater. 307, 237-244.

Pamme, N., Manz, A., 2004. On-chip free-flow magnetophoresis: Continuous flow separation of magnetic particles and agglomerates. Anal. Chem. 76, 7250-7256.

Pamme, N., Wilhelm, C., 2006. Continuous sorting of magnetic cells via on-chip free-flow magnetophoresis. Lab Chip 6, 974-980.

Pankhurst, Q.A., Connolly, J., Jones, S.K., Dobson, J., 2003. Applications of magnetic nanoparticles in biomedicine. J. Phys. D: Appl. Phys. 36, R167-R181.

Verpoorte, E., 2003. Beads and chips: new recipes for analysis. Lab Chip 3, 60N-68N.

Xia, N., Hunt, T.P., Mayers, B.T., Alsberg, E., Whitesides, G.M., Westervelt, R.M., Ingber, D.E., 2006. Combined microfluidic-micromagnetic separation of living cells in continuous flow. Biomed. Microdev. 8, 299-308.